BRL

REPORT NO. 1225
OCTOBER 1963

431846

THE UNSTEADY FLOW WITHIN A SPINNING CYLINDER

E. H. Wedemeyer

RDT & E Project No. 1M010501A005

BALLISTIC RESEARCH LABORATORIES

ABERDEEN PROVING GROUND, MARYLAND

This report is expected to appear in Journal of Fluid Mechanics.

DDC AVAILABILITY NOTICE

Qualified requesters may obtain copies of this report from DDC.

The findings in this report are not to be construed as an official Department of the Army position.

BALLISTIC RESEARCH LABORATORIES

REPORT NO. 1225

OCTOBER 1963

THE UNSTEADY FLOW WITHIN A SPINNING CYLINDER

E. H. Wedemeyer

Exterior Ballistics Laboratory

RDT & E Project No. 1M010501A005

ABERDEEN PROVING GROUND, MARYLAND

B A L L I S T I C R E S E A R C H L A B O R A T O R I E S

REPORT NO. 1225

EHWedemeyer/bj
Aberdeen Proving Ground, Md.
October 1963

THE UNSTEADY FLOW WITHIN A SPINNING CYLINDER

ABSTRACT

A theoretical analysis is given of the unsteady flow within a liquid-filled cylinder of finite length, which is started impulsively to spin about its axis.

It is established that a secondary flow, which is caused by the cylinder ends, has a remarkable effect on the generation of spin in the liquid.

The theoretical results are compared with experimental observations and good agreement is found.

TABLE OF CONTENTS

I. INTRODUCTION

It is well known that spin-stabilized shells can become dynamically unstable if they are filled with a liquid. According to a theoretical analysis of K. Stewartson (1959), the stability of a shell containing a cylindrical liquid-filled cavity can be predicted if the liquid is in rigid body rotation.

However, for a liquid of small viscosity, it requires a relatively long time for the liquid to reach full spin, and, during the transition period, the shell might become dynamically unstable even though it might be stable at its final state if the liquid attained rigid body rotation. In the course of experimental investigations (B. G. Karpov, 1962), severe dynamic instabilities of liquid-filled spinning shells have been observed in cases where the shell should have been stable according to Stewartson's theory and the assumption of rigid rotation of the liquid filler. In order to extend the prediction of instabilities in such cases, it appeared desirable to analyze the problem of unsteady fluid motion within a cylinder, started to spin about its axis.

If the cylinder is infinitely long, a solution to the problem is obtained without difficulty, but the expectation that this solution might approximately be valid for slender but finite cylinders proves to be wrong. It is found that the effect of the cylinder ends on the fluid motion is not only not negligible, but dominating. The fluid motion is entirely changed by the presence of a secondary flow induced by the cylinder ends. The secondary flow convects spinning fluid from the walls into the interior of the cylinder and, as a consequence, the fluid attains rotational motion many times faster than without secondary flow. In the following, a theoretical analysis is given of the unsteady flow within a cylinder which is started to spin about its axis of rotation. The results are then compared with some experimental data obtained: 1) from spin decay data of liquid-filled shells; and 2) from direct observations of the secondary flow within a spinning transparent cylinder.

II. THEORETICAL ANALYSIS OF THE FLOW

a. Structure of the Secondary Flow

The diagram in Figure 1 shows an axial section and a cross-section of the spinning cylinder. The height of the cylinder is h, the radius a. For the following analysis, we use a polar-coordinate system θ, r, z with the origin in the center as shown in the diagram (Figure 1). The velocity components are v, u, w, respectively. The Navier-Stokes equations in these coordinates for a flow of rotational symmetry are:

$$\frac{\partial v}{\partial t} + u\left(\frac{\partial v}{\partial r} + \frac{v}{r}\right) + w\frac{\partial v}{\partial z} = \nu\left[\frac{\partial^2 v}{\partial r^2} + \frac{\partial}{\partial r}\left(\frac{v}{r}\right) + \frac{\partial^2 v}{\partial z^2}\right] \tag{1a}$$

$$\frac{\partial u}{\partial t} + u\frac{\partial u}{\partial r} + w\frac{\partial u}{\partial z} - \frac{v^2}{r} + \frac{1}{\rho}\frac{\partial p}{\partial r} = \nu\left[\frac{\partial^2 u}{\partial r^2} + \frac{\partial}{\partial r}\left(\frac{u}{r}\right) + \frac{\partial^2 u}{\partial z^2}\right] \tag{1b}$$

$$\frac{\partial w}{\partial t} + u\frac{\partial w}{\partial r} + w\frac{\partial w}{\partial z} + \frac{1}{\rho}\frac{\partial p}{\partial z} = \nu\left[\frac{\partial^2 w}{\partial r^2} + \frac{1}{r}\frac{\partial w}{\partial r} + \frac{\partial^2 w}{\partial z^2}\right] \tag{1c}$$

$$\frac{\partial ru}{\partial r} + \frac{\partial rw}{\partial z} = 0 \tag{1d}$$

The boundary conditions are $u = w = 0$, $v = r\omega$ at $z = \pm h/2$, and $u = w = 0$, $v = a\omega$ at $r = a$, with $u = 0$ at $r = 0$.

Let us assume the cylinder is started at time $t = 0$ to spin about its axis of rotation with the constant or time-dependent angular velocity ω.

If the cylinder is infinitely long; i.e., $h \to \infty$, the Equations (1b), (1c) and (1d) with the corresponding boundary conditions are solved by

$$u = w = 0, \quad \frac{\partial p}{\partial z} = 0, \quad \frac{1}{\rho}\frac{\partial p}{\partial r} = \frac{v^2}{r}$$

and Equation (1a) reduces to a linear differential equation:

$$\frac{\partial v}{\partial t} = \nu\left(\frac{\partial^2 v}{\partial r^2} + \frac{\partial v/r}{\partial r}\right), \tag{2}$$

where v depends on r and t only; i.e., $v(r,t)$. No such solution with $u = w = 0$ is possible if the cylinder has a finite length. In the vicinity of the endwalls, $z = \pm h/2$, the circumferential component v must depend on z and, according to Equations (1b) and (1c), the velocity components u, w must be different from zero. In fact, the fluid particles at the cylinder ends rotate with the velocity of the walls and, therefore, are subject to centrifugal forces. Due to these centrifugal forces, the particles close to the endwalls are driven outward, creating a secondary flow with velocity components u, w. We can assume, however, with the reservation of a final proof, that the secondary motion u, w is very slow except in a thin boundary layer region at each of the endwalls. Thus, we can divide the entire flow region in two parts, the boundary layer region close to the endwalls and the rest of the flow, which we will call the core flow. A similar flow structure was found by Ludwieg (1951) for the steady flow in a rotating duct, and the following considerations will be analogous to those given by Ludwieg (1951).

b. Approximate Equation for the Core Flow

Let us use the notation v_o, u_o, w_o, p_o for the velocity components and the pressure in the core flow. If we apply Equation (1b) to the core flow, we can neglect the terms containing u, w, according to our assumption that the secondary motion is very slow in the core flow, and we have approximately

$$\frac{1}{\rho}\frac{\partial p_o}{\partial r} = \frac{v_o^2}{r} \quad . \tag{3}$$

From Equation (1c) we observe that the axial pressure gradient $\frac{\partial p_o}{\partial z}$ is very small; or, within our approximation, we can assume that the pressure is independent of z. But then, according to Equation (3), v_o must be independent of z, and Equation (1a) applied to the core flow gives:

$$\frac{\partial v_o}{\partial t} + u_o\left(\frac{\partial v_o}{\partial r} + \frac{v_o}{r}\right) = \nu\left(\frac{\partial^2 v_o}{\partial r^2} + \frac{\partial v_o/r}{\partial r}\right) \quad . \tag{4}$$

Since v_o is independent of z, it can be seen from Equation (4) that also u_o must be independent of z. Thus, Equation (4) reduces to a partial differential equation in the independent variables r and t.

Before we can solve Equation (4) for the circumferential component v_o, we must have an additional relation which allows us to express the other dependent variable u_o by v_o. The required additional relation between u_o and v_o will be given by the coupling between boundary layer flow and core flow.

c. Boundary Layer Flow

Since the flow within the spinning cylinder must be symmetric with respect to the middle plane z = 0, we can restrict our analysis to the boundary layer at one of the endwalls, say z = - h/2.

The boundary layer equations can be obtained from the Navier-Stokes Equations (1a) to (1d), applying the usual boundary layer simplifications. The radial pressure gradient within the boundary layer can be replaced by the pressure gradient of the "outer" flow; i.e., the core flow in our case. Thus, according to Equation (3), $\frac{1}{\rho}\frac{\partial p}{\partial r} = v_o^2/r$. The friction forces reduce to $\nu\frac{\partial^2 v}{\partial z^2}$, etc. Although the boundary layer flow is unsteady, we can treat it as a quasi-steady flow; i.e., the local acceleration terms $\frac{\partial v}{\partial t}$, etc., can be neglected. Apart from a very short acceleration period, after the cylinder is started to spin, the local acceleration terms are very small compared to the convective terms. During the acceleration period, the flow at each of the endwalls is

essentially the same as the flow on an impulsively started rotating disk. The unsteady boundary layer flow on an impulsively started rotating disk was investigated by Thiriot (1940). According to Thiriot's solution, the duration of the acceleration period is about $t \approx \frac{2}{\omega}$; i.e., after a fraction $\frac{1}{\pi}$ of a revolution the boundary layer flow is almost steady. We can, therefore, ignore the acceleration period and consider the boundary layer flow as quasi-steady for all time. The boundary layer equations then are:

$$u \frac{\partial u}{\partial r} + w \frac{\partial u}{\partial z} - \frac{v^2}{r} + \frac{v_o^2}{r} = \nu \frac{\partial^2 u}{\partial z^2} \tag{5a}$$

$$u \frac{\partial v}{\partial r} + u \frac{v}{r} + w \frac{\partial v}{\partial z} = \nu \frac{\partial^2 v}{\partial z^2} \tag{5b}$$

$$\frac{\partial ru}{\partial r} + \frac{\partial rw}{\partial z} = 0 \tag{5c}$$

For convenience we change our coordinate system, so that the lower endwall of the cylinder is given by $z = 0$. The boundary conditions, then, are:

$$\left.\begin{aligned} v &= r\omega \\ u &= 0 \\ w &= 0 \end{aligned}\right\} \text{ at } z = 0$$
$$\left.\begin{aligned} v &= v_o(r,t) \\ u &= 0 \end{aligned}\right\} \text{ at } z = \infty \tag{5d}$$

v_o enters into our boundary layer problem twice; first, it occurs in Equation (5a); and secondly, it enters into one of the boundary conditions. For any given outer flow $v_o(r)$, the boundary layer flow is determined by the Equations (5a, b, c) and the boundary conditions (5d). Thus, we have a coupling between the boundary layer flow and the core flow.

The boundary layer Equations (5a, b, c) have been the subject of many investigations. von Kármán (1921) considered the flow on a rotating disk in a fluid at rest ($v_o = 0$) and obtained approximate solutions using the integral method he invented. A more accurate solution to the same problem was calculated by Cochran (1934). The problem of rigid body fluid rotation over a stationary disk was solved by Bödewadt (1940).

Batchelor (1951), Stewartson (1958), Rogers and Lance (1960) and others investigated the more general problem of a fluid in rigid body rotation over a rotating disk. A common feature of the above mentioned flows is that they have

similarity solutions, where the velocity components take the form $v = r\,G(z)$, $u = r\,F(z)$, $w = H(z)$. These similarity solutions are also solutions of the exact Navier-Stokes equations, since the terms, which are commonly neglected in boundary layer theory, vanish identically. Ludwieg (1951) and Squire (1953) linearized the boundary layer Equations (5a, b, c) for the case of small disturbances about a state of rigid rotation. In the linearized form, the Equations (5a, b, c) reduce to a set of ordinary differential equations, which are linear.

For general v_o - distributions, when neither linearization nor the assumption of similarity flow is applicable, approximate solutions may be obtained by using the momentum integral method. Mack (1962) (1963) has applied the momentum integral method (1962) and a simplified momentum integral method (1963) to rotating flows on a stationary disk. The latter method, which makes computations easy, could be extended to our case of rotating flows on a rotating disk.

While the momentum integral method does not give the exact shape of the velocity profiles, it provides fairly good approximations to certain integral values, e.g., the radial mass flow within the boundary layer, which is

$$M(r) = 2\pi r \cdot \rho \int_0^{\delta} u(r,z)\,dz \quad \text{where } \delta \text{ is the boundary layer}$$

thickness. When the radial mass flow distribution $M(r)$ has been determined - for a given distribution of $v_o(r)$ - the radial velocity in the core flow, $u_o(r)$, can be found.

Making use of the condition, that the total radial mass flow (within the two boundary layers and the core flow) must be zero, one obtains

$$2\pi r \cdot \rho \left[2 \int_0^{\delta} u(r,z)\,dz + h\,u_o(r) \right] = 0 \tag{6}$$

or

$$-\frac{h}{2}\,u_o(r) = \int_0^{\delta} u(r,z)\,dz$$

Thus, we have a functional dependence

$$u_o(r) = F[v_o(r)] \tag{7}$$

This means, for any given distribution of $v_o(r)$ we can find the distribution of $u_o(r)$.

In principle we could now express u_o in Equation (4) by v_o making use of the functional dependence (7). But aside from the fact that we cannot give an explicit formula for $u_o(r)$, the relation (7) will be much too complex to enable us to solve Equation (4). Thus we have to confine ourselves to a simple approximation of the relation (7).

d. Approximate Formula for $u_o(r)$

At the beginning of the fluid motion the circumferential component of the core flow, v_o, is zero and the boundary layer problem reduces to the problem of the rotating disk flow, which was solved by Cochran (1934).

According to Cochran's solution we have:

$$\int_0^\infty u\,dz = 0.443\sqrt{\frac{\nu}{\omega}}\ .\ (r\omega) \tag{8}$$

and hence, from Equation (6)

$$-\frac{h}{2}u_o = 0.443\sqrt{\frac{\nu}{\omega}}\ r\omega \tag{9}$$

If on the other hand the fluid finally attains the state of rigid rotation ($v_o = r\omega$) the boundary layer Equations (5) have the trivial solution $v = r\omega$, $u = w = 0$ and hence $u_o = 0$.

The simplest possible approximation for general v_o distributions then is to assume, that:

$$-\frac{h}{2}u_o = 0.443\sqrt{\frac{\nu}{\omega}}\ (r\omega - v_o), \tag{10}$$

which is a linear interpolation between the two extreme cases.

We can test the validity of this approximation in a few other cases. If the core flow is almost a rigid body rotation with the angular velocity ω, i.e., $v_o = r\omega + v_o'$ and $|v_o'| << r\omega$, the boundary layer Equations (5a, b, c) can be linearized. In doing this we transform:

$$\begin{aligned} v_o &= r\omega + v_o';\ u = u' \\ v &= r\omega + v';\ w = w' \end{aligned} \tag{11}$$

where the primed quantities are small compared with $r\omega$. Substituting (11) into (5a, b) and neglecting terms of higher than first order in the primed quantities, Equations (5a, 5b) become:

$$\nu \frac{\partial^2 v'}{\partial z^2} - 2\omega u' = 0$$

$$\nu \frac{\partial^2 u'}{\partial z^2} + 2\omega (v' - v_o') = 0 \qquad (12)$$

These linearized equations were used by Ludwieg (1951) for the boundary layer flow in a rotating duct.

With the boundary conditions:

$$\left.\begin{aligned} v' &= 0 \\ u' &= 0 \end{aligned}\right\} \text{at } z = 0 \qquad \left.\begin{aligned} v' &= v_o' \\ u' &= 0 \end{aligned}\right\} \text{at } z = \infty$$

Equations (12) are solved by:

$$v' = v_o' \left(1 - \cos\sqrt{\frac{\omega}{\nu}}\, z \cdot e^{-\sqrt{\frac{\omega}{\nu}}\, z}\right)$$

$$u' = - v_o' \sin\sqrt{\frac{\omega}{\nu}}\, z \cdot e^{-\sqrt{\frac{\omega}{\nu}}\, z} \qquad (13)$$

For the radial component in the core flow u_o we have, according to Equation (6)

$$-\frac{h}{2} u_o(r) = \int_o^\infty u' dz = - v_o' \sqrt{\frac{\nu}{\omega}} \cdot \frac{1}{2}$$

If we replace v_o' according to (11) by $-(r\omega - v_o)$, we have:

$$-\frac{h}{2} u_o = 0.500 \cdot \sqrt{\frac{\nu}{\omega}} (r\omega - v_o) \qquad (14)$$

This formula for u_o is similar to the linear interpolation formul (10) except that the factor of 0.500 in (14) is 13% larger than the factor 0.443 in (10), so that the error of the approximate formula (10) in this case is 13%.

For the case that the outer flow is a rigid rotation with the angular velocity Ω, i.e., $v_o = r\Omega$, the boundary layer Equations (5) have been solved by Rogers and Lance (1960) for several values of $\frac{\Omega}{\omega}$.

According to the solution of Rogers and Lance (1960), the radial flow integral is given by:

$$-\frac{h}{2}u_o = \int_o^\infty u\,dz = \sqrt{\frac{\nu}{\omega}} \cdot r\omega\, f\left(\frac{\Omega}{\omega}\right) \qquad (15)$$

where the function $f(\frac{\Omega}{\omega})$ is shown in Figure 2. If we apply our approximation formula (10) to the case, when $v_o = r\Omega$, we get:

$$-\frac{h}{2}u_o = \sqrt{\frac{\nu}{\omega}} \cdot r\omega \cdot 0.443\left(1 - \frac{\Omega}{\omega}\right)$$

Thus the function $f(\frac{\Omega}{\omega})$ has to be compared with the approximate expression $0.443\,(1 - \frac{\Omega}{\omega})$, which is shown by the dotted line in Figure 2.

The agreement is still good enough that we can consider Equation (10) as a reasonable approximation also in this case. Whether or not Equation (10) is approximately valid for the actual velocity profiles $v_o(r,t)$ can be checked after obtaining the solution for $v_o(r,t)$. A calculation of the radial flow integral for some of the obtained velocity profiles $v_o(r,t)$ has been done, based on the simplified momentum integral method of Mack (1963). The u_o values obtained from these calculations have been compared with the approximate values from Equation (10) and the agreement was found to be good within the accuracy of the momentum integral method, which is about 15%. Thus, we can conclude this section with the remark that the error of the approximation for u_o (Equation 10) is probably not larger than 15%.

Using the notation $Re = \frac{a^2\omega}{\nu}$ for the Reynolds number, Equation (10) can be written:

$$u_o = -0.443\,\frac{2a}{h} \cdot \frac{1}{\sqrt{Re}}\,(r\omega - v_o) \qquad (17)$$

or, with the notation

$$k = 0.443\,\frac{2a}{h}\frac{1}{\sqrt{Re}} \qquad (18)$$

$$u_o = -k\,(r\omega - v_o) \qquad (19)$$

e. Solution for $v_o(r,t)$

After substituting (19) into Equation (4) the equation for v_o is:

$$\frac{\partial v_o}{\partial t} + k(v_o - r\omega)\left(\frac{\partial v_o}{\partial r} + \frac{v_o}{r}\right) = \nu\left(\frac{\partial^2 v_o}{\partial r^2} + \frac{\partial v_o/r}{\partial r}\right) \qquad (20)$$

where $k = 0.443 \frac{2a}{h} \cdot \frac{1}{\sqrt{Re}}$.

The initial and boundary conditions are

$$v_o = 0 \quad \text{for } t < 0$$

$$v_o = a\omega \text{ for } r = a \text{ and } t \geq 0$$

Let us restrict our analysis at this instant to the case of constant ω (i.e., the cylinder is started at $t = 0$ to spin with constant angular velocity ω). In many cases now, we can neglect the friction terms at the right hand side of Equation (20) against the convection terms. To see this, we multiply Equation (20) with $\frac{1}{a\omega^2}$ and, introducing the dimensionless variables $v^* = \frac{v_o}{a\omega}$, $r^* = \frac{r}{a}$ Equation (20) becomes:

$$\frac{\partial v^*}{\partial \omega t} + k(v^* - r^*)\left(\frac{\partial v^*}{\partial r^*} + \frac{v^*}{r^*}\right) = \frac{1}{Re}\left(\frac{\partial^2 v^*}{\partial r^{*2}} + \frac{\partial}{\partial r^*}\frac{v^*}{r^*}\right) \qquad (21)$$

with the boundary conditions:

$$v^* = 1 \text{ for } r^* = 1 \text{ and } \omega t \geq 0$$

It can be seen from Equation (21) that the solution v^* is a function of $k\omega t$, r^* and the dimensionless parameter $kRe = 0.443 \frac{2a}{h} \cdot \sqrt{Re}$, i.e., $v^* = f(r^*, k\omega t, kRe)$.

If $kRe = 0.443 \cdot \frac{2a}{h}\sqrt{Re} >> 1$ then the viscous terms at the right hand side of (21) become small except for small times when the gradient $\frac{\partial v^*}{\partial r^*}$ is large near the wall $r^* = 1$.

For not too small times and $kRe >> 1$ we can therefore neglect the viscous terms and the solution of the inviscid equation is:

$$v^* = \frac{r^* e^{2k\omega t} - \frac{1}{r^*}}{e^{2k\omega t} - 1} \quad \text{for } r^* \geq e^{-k\omega t}$$

$$v^* = 0 \qquad \text{for } r^* \leq e^{-k\omega t} \qquad (22)$$

A plot of the v^* profiles (Equation 22) for different times is shown in Figure 3.

It is remarkable that the solution (22) satisfies also the complete Equation (21) with viscous terms except at the point $r^* = e^{-k\omega t}$ where the first derivative is discontinuous. The inviscid equation is of the first order in the

derivatives and hence only the solution function has to be continuous, while the complete equation has second order derivatives and the solution must have continuous derivatives. The effect of the viscosity, therefore, will be to smooth the corner at $r^* = e^{-k\omega t}$. With the solution for v_o (Equation 22) the other flow components u_o, w_o can be obtained at once. First of all we have, from Equation (19):

$$u_o = -k(r\omega - v_o).$$

From the equation of continuity (Equation 1d) and the condition that the flow must be symmetric to the plane $z = 0$, it follows:

$$w_o = -\frac{2}{r}\frac{\partial r u_o}{\partial r}. \qquad (23)$$

Within the core flow we can distinguish two regions:

Region (1): $0 < r/a < e^{-k\omega t}$

Region (2): $e^{-k\omega t} < r/a < 1$

According to Equation (22) the particles in region (1) do not rotate (i.e., $v_o = 0$) while the particles in region (2) rotate with the velocity $v_o = a\omega r^*$ given by Equation (22). Region (1) and (2) are separated by the cylindrical front $r/a = e^{-k\omega t}$, which is moving toward the axis $r = 0$.

It can be shown that the particles in region (1), i.e., the particles ahead of the moving front, remain ahead of it until they hit one of the boundary layers at the endwalls $z = \pm \frac{h}{2}$.

To see this, we compute the trajectories of the particles in region (1). From $v_o = 0$ it follows, that $u_o = -kr\omega$ and $w_o = -2kz\omega$ (Equation 23). From:

$$\frac{dr}{dt} = u_o = -kr\omega$$
$$\frac{dz}{dt} = w_o = 2kz\omega \qquad (24)$$

we obtain by integration:

$$r = r_o e^{-k\omega t}$$
$$z = z_o e^{2k\omega t} = z_o\left(\frac{r_o}{r}\right)^2 \qquad (25)$$

where (r_o, z_o) is the particle position at $t = 0$.

The trajectories (25) course entirely in region (1), so that the solution (25) is compatible with the supposition $v_o = 0$.

Thus, we obtain the following flow picture:

After the cylinder is started at t = 0, the fluid particles move along hyperbolas given by (25) until they hit the boundary layer at one of the endwalls $z = \pm \frac{h}{2}$.

In the boundary layer the flow direction changes rapidly, the particles acquire rotational motion and are thrown radially outwards until they emerge from the boundary layer at some distance behind the moving front $r/a = e^{-k\omega t}$, now having a rotational component v_o according to Equation (22). The rest of the trajectory courses entirely in region (2).

Actually, this flow picture will be modified slightly. The particles can acquire rotational motion already in region (1) by the action of the viscous force term in Equation (21) which has been neglected so far. This will also slightly modify the trajectories given by Equation (25).

f. Equations for the Angular Momentum

Of particular interest is the total angular momentum of the liquid within the cylinder, which is:

$$I = \rho h \cdot 2\pi \int_0^a r^2 v_o \, dr \tag{26}$$

An equation for the angular momentum I can be obtained from Equation (20).

To this end, we multiply Equation (20) by r^2 and integrate from r = 0 to r = a. If we consider that $\frac{\partial v_o}{\partial r} + \frac{v_o}{r} = \frac{1}{r}\frac{\partial r v_o}{\partial r}$, this gives:

$$\left[\frac{\partial}{\partial t}\int_0^a r^2 v_o \, dr + k\int_0^a (r v_o - r^2\omega)\frac{\partial r v_o}{\partial r}\, dr\right] = \left[\nu \int_0^a r^2 \frac{\partial}{\partial r}\left(\frac{1}{r}\frac{\partial r v_o}{\partial r}\right) dr\right] \tag{27}$$

The second integral consists of two terms: the first one gives:

$$k\int_0^a r v_o \frac{\partial r v_o}{\partial r}\, dr = \left[\frac{k}{2}(r v_o)^2\right]_0^a$$

while the second term can be integrated by parts:

$$-k\omega \int_0^a r^2 \frac{\partial r v_o}{\partial r}\, dr = \left[-k\omega r^3 v_o\right]_0^a + 2k\omega \int_0^a r^2 v_o \, dr$$

Considering that $v_o = a\omega$ for $r = a$, the second integral of Equation (27) gives:

$$k\int (rv_o - r^2\omega)\frac{\partial rv_o}{\partial r}\,dr = -\frac{k}{2}a^4\omega^2 + 2k\omega\int_o^a r^2 v_o\,dr$$

The integral at the right side of Equation (27) becomes, after integration by parts:

$$\nu\int_o^a r^2\frac{\partial}{\partial r}\left(\frac{1}{r}\frac{\partial rv_o}{\partial r}\right)dr = \nu\left[r\frac{\partial rv_o}{\partial r}\right]_o^a - \nu[2rv_o]_o^a = \nu a^3\left(\frac{\partial v_o/r}{\partial r}\right)_{r=a}$$

We thus get the equation:

$$\frac{d}{dt}\int_o^a r^2 v_o\,dr - \frac{k}{2}a^4\omega^2 + 2k\omega\int_o^a r^2 v_o\,dr = \nu a^3\left(\frac{\partial v_o/r}{\partial r}\right)_{r=a} \qquad (28)$$

According to (26) the value of the angular momentum is : $I = 2\pi h\,.\,\rho\int_o^a r^2 v_o\,dr.$

In the final state, i.e., when the liquid approaches rigid body rotation $v_o = r\omega$, the angular momentum becomes:

$$I_\infty = 2\pi h\,.\,\rho\int_o^a r^3\omega\,dr = 2\pi h\,.\,\rho\,.\,\frac{a^4\omega}{4} \qquad (29)$$

The ratio of the angular momentum I to its final value I_∞, then is:

$$\frac{I}{I_\infty} = \frac{\int_o^a r^2 v_o\,dr}{a^4\omega/4}$$

After dividing Equation (28) by $\frac{a^4\omega}{4}$, it can be written:

$$\frac{d}{dt}\left(\frac{I}{I_\infty}\right) + 2k\omega\left[\frac{I}{I_\infty} - 1\right] = \frac{4\nu}{a\omega}\left(\frac{\partial v_o/r}{\partial r}\right)_{r=a} \qquad (30)$$

If we neglect again the viscous term at the right side of Equation (30), the equation can be integrated at once to give:

$$\frac{I}{I_\infty} = (1 - e^{-2k\omega t}) \qquad (31)$$

This result, of course, could have been obtained also from the solution Equation (22) for the velocity profiles $v^* = \frac{v_o}{a\omega}$ by integration.

In order to improve the solution (31) we have to take into account the friction term $\frac{4\nu}{a\omega}\left(\frac{\partial v_o/r}{\partial r}\right)_{r=a}$ of Equation (30). This can be done within a fairly good approximation by assuming the approximate shape of the velocity profiles $v_o(r)$ and expressing $\left(\frac{\partial v_o/r}{\partial r}\right)_{r=a}$ by I/I_∞.

Since the contribution of the viscous term is small, it appears reasonable to assume that the v_o profiles have essentially the same shape as the profiles, which we have obtained as solution for the inviscid equation.

Thus, we may assume profiles of the form:

$$\begin{aligned} \frac{v_o}{a\omega} &= \frac{A^2 \cdot r/a - a/r}{A^2 - 1} \quad \text{for } r/a > A^{-1} \\ \frac{v_o}{a\omega} &= 0 \qquad\qquad\qquad \text{for } r/a < A^{-1} \end{aligned} \tag{32}$$

where A is a function of time. For the case that the viscous term is neglected at all, the solution for $\frac{v_o}{a\omega}$ was given, according to Equation (22), by the profiles (32) with $A = e^{k\omega t}$.

It might be mentioned, that the v_o profiles (32) satisfy the compatibility condition

$$\left(\frac{\partial^2 v_o}{\partial r^2} + \frac{\partial v_o/r}{\partial r}\right)_{r=a} = 0 \tag{33}$$

which is obtained by evaluating Equation (20) at r=a. Using the v_o profiles given by (32) we have:

$$\left(\frac{\partial v_o/r}{\partial r}\right)_{r=a} = \frac{2\omega}{a} \cdot \frac{1}{A^2 - 1} \tag{34}$$

while

$$I/I_\infty = 1 - A^{-2} \tag{35}$$

Thus, from (34) and (35) we obtain:

$$\left(\frac{\partial v_o/r}{\partial r}\right)_{r=a} = \frac{2\omega}{a}\left[\frac{1}{I/I_\infty} - 1\right] \tag{36}$$

Inserting (36) into (30) we have:

$$\frac{d}{dt}\left(\frac{I}{I_\infty}\right) + 2k\omega\left[\frac{I}{I_\infty} - 1\right] = \frac{8\nu}{a^2}\left[\frac{1}{I/I_\infty} - 1\right]$$

or, after dividing by ω,

$$\frac{dI/I_\infty}{d\omega t} + 2k\left[\frac{I}{I_\infty} - 1\right] = \frac{8}{Re}\left[\frac{1}{I/I_\infty} - 1\right] \tag{37}$$

It should be mentioned that the approximation for $\left(\frac{\partial v_o/r}{\partial r}\right)_{r=a}$, which is given by Equation (36), is not very sensitive to the special choice of velocity profiles. Although the very early v_o profiles are somewhat different from those given in Equation (32), the expression (36) is still a good approximation.

It can be obtained from Equation (37) that for sufficiently small times the friction term is dominant however large kRe is.

The equation for v_o then is:

$$\frac{\partial v_o}{\partial t} = \nu \frac{\partial^2 v_o}{\partial r^2} \tag{38}$$

which is obtained from Equation (20) by neglecting the convection terms and $\nu \frac{\partial v_o/r}{\partial r}$ compared with $\nu \frac{\partial^2 v_o}{\partial r^2}$.

The solution of (38) is:

$$v_o(r,t) = a\omega\left[1 - \frac{2}{\sqrt{\pi}} \int_0^{\frac{a-r}{\sqrt{\nu t}}} e^{-y^2}\, dy\right] \tag{39}$$

With the velocity profiles given by Equation (39) one would have:

$$\left(\frac{\partial v_o/r}{\partial r}\right)_{r=a} = \frac{8}{\pi} \cdot \frac{\omega}{a} \cdot \frac{1}{I/I_\infty} = 2.54 \frac{\omega}{a} \cdot \frac{1}{I/I_\infty}$$

while Equation (36) gives approximately

$$\left(\frac{\partial v_o/r}{\partial r}\right)_{r=a} = 2 \frac{\omega}{a} \frac{1}{I/I_\infty}$$

since for small times we can neglect 1 against $\frac{1}{I/I_\infty}$. Thus, we see that Equation (36) is a reasonably good approximation even for the very early velocity profiles.

The differential Equation (37) now has to be solved for the initial condition $I/I_\infty = 0$ at $t = 0$. The solution for I/I_∞ can be given implicitly:

$$2k\omega t = \frac{-1}{1 + \frac{4}{kRe}} \left[\log (1 - I/I_\infty) + \frac{4}{kRe} \log \left(1 + \frac{kRe}{4} I/I_\infty\right)\right] \qquad (40)$$

For $kRe \to \infty$ the solution (40) reduces to: $1 - I/I_\infty = e^{-2k\omega t}$; i.e., the inviscid solution given by (31).

For very small times, or more precisely for $I/I_\infty << 1$ and $\frac{kRe}{4} I/I_\infty << 1$, Equation (40) gives: $I/I_\infty \approx \frac{4}{\sqrt{Re}} \cdot \sqrt{\omega t}$; i.e., the angular momentum increases as the square root of t.

The validity of the preceding results is restricted to the case where the angular velocity of the cylinder, ω, remains constant after the cylinder is started.

If ω is not constant, it is advantageous to introduce the dimensionless quantity

$$I^* = \frac{I}{I_o} = \frac{4}{a^4 \omega_o} \int_o^a v_o r^2 dr, \qquad (41)$$

where ω_o is a constant reference angular velocity and I_o is a reference angular momentum:

$$I_o = 2\pi \rho h \int_o^a \omega_o r^3 dr,$$

the latter corresponding to a rigid rotation with angular velocity ω_o.

Dividing Equation (28) by $\frac{a^4 \omega_o^2}{4}$ and substituting $\left(\frac{\partial v_o/r}{\partial r}\right)_{r=a}$ according to Equation (36) we have:

$$\frac{dI^*}{d\omega_o t} + 2k_o \left(\frac{\omega}{\omega_o}\right)^{1/2} \left[I^* - \frac{\omega}{\omega_o}\right] = \frac{8}{Re_o} \frac{\omega}{\omega_o} \left[\frac{1}{I^*} \frac{\omega}{\omega_o} - 1\right] \qquad (42)$$

where: $Re_o = \frac{a^2 \omega_o}{\nu}$ and $k_o = 0.443 \frac{2a}{h} \cdot (Re_o)^{-1/2}$

Equation (42) has been used to calculate the spin decay of a liquid-filled shell. If a shell containing a liquid-filled cylindrical cavity is started impulsively to spin about its axis of rotation, the liquid continuously absorbs angular momentum, thus reducing the spin until the liquid finally attains rigid body rotation.

Let A be the axial moment of inertia of the empty shell, ω the instantaneous angular velocity and I the angular momentum of the liquid, then, due to the conservation of angular momentum,

$$I + \omega A = \text{constant} = \omega_o A, \tag{43}$$

where ω_o is the initial angular velocity when the liquid is at rest.

According to (43) we can express I by ω:

$$I = A\omega_o(1 - \omega/\omega_o),$$

or using the definition (41):

$$I^* = \frac{A\omega_o}{I_o}(1 - \omega/\omega_o). \tag{44}$$

After inserting (44) into (42) we get a differential equation for I^* (or ω/ω_o) which may be solved by numerical integration.

g. Turbulent Boundary Layer Flow

In Sections (c) and (d) we have assumed that the boundary layer flow at the cylinder ends is laminar. This assumption is valid for Reynolds numbers $Re = \frac{a^2\omega}{\nu}$ up to about $3 \cdot 10^5$ (see e.g. Schlichting 1958). For Reynolds numbers greater than $3 \cdot 10^5$ the boundary layer flow will be turbulent and the radial mass flow and hence u_o will be different from the laminar case.

According to the solution of von Kármán (1921) for the turbulent boundary layer flow on a rotating disk, the radial flow integral is:

$$\int_0^\infty u\,dz = 0.035\, r^{3/5}\left(\frac{\nu}{\omega}\right)^{1/5} r\omega \tag{45}$$

This formula is analogous to Equation (8), which corresponds to the laminar case.

Using again the notation $Re = \frac{a^2\omega}{\nu}$ for the Reynolds number, Equation (45) can be written:

$$\int_0^\infty u\,dz = 0.035\, a\, .\, (Re)^{-1/5}\, \frac{(r\omega)^{8/5}}{(a\omega)^{3/5}} \tag{46}$$

By arguments similar to those used in Section (d) for the laminar boundary layer, it seems appropriate to generalize Equation (46) to:

$$\int_0^\infty u\,dz = 0.035\, a\, .\, (Re)^{-1/5}\, \frac{(r\omega - v_o)^{8/5}}{(a\omega)^{3/5}} \tag{47}$$

According to Equation (6) we then have for the radial component of the core flow:

$$u_o(r) = - 0.035 \cdot \left(\frac{2a}{h}\right) \cdot (Re)^{-1/5} \frac{(r\omega - v_o)^{8/5}}{(a\omega)^{3/5}} \qquad (48)$$

Equation (48) is analogous to Equation (17). With u_o obtained from Equation (48) the equation for the core flow (Equation 4) becomes:

$$\frac{\partial v_o}{\partial t} - \frac{k_t}{(a\omega)^{3/5}} (r\omega - v_o)^{8/5} \left(\frac{\partial v_o}{\partial r} + \frac{v_o}{r}\right) = \nu \left[\frac{\partial^2 v_o}{\partial r^2} + \frac{\partial v_o/r}{\partial r}\right] \qquad (49)$$

where:

$$k_t = 0.035 \left(\frac{2a}{h}\right) (Re)^{-1/5} \qquad (50)$$

Analogous to the procedure described in Section (f), we find the equation for the angular momentum by multiplying Equation (49) with $r^2 \cdot \frac{4}{a^4 \omega_o^2}$ and integrating over r.

If we further introduce again the dimensionless quantity I* according to Equation (41) we finally have:

$$\frac{dI^*}{d\omega_o t} - \frac{k_t}{(a\omega)^{3/5}} \frac{4}{a^4 \omega_o^2} \int_o^a r(r\omega - v_o)^{8/5} \left(\frac{\partial r v_o}{\partial r}\right) dr = \frac{4\nu}{a\omega_o} \left(\frac{\partial v_o/r}{\partial r}\right)_{r=a} \qquad (51)$$

The integral in Equation (51) cannot be evaluated as it could for the laminar case, without knowing how v_o depends on r. Only for small times when the v_o profiles are restricted to a narrow zone near the wall r=a, we can approximate r in the integral by a and find:

$$\int_o^a a(a\omega - v_o)^{8/5} \frac{\partial a v_o}{\partial r} dr = \left[\frac{5}{13} a^2 (a\omega - v_o)^{13/5}\right]_o^a = \frac{5}{13} a^2 (a\omega)^{13/5}$$

Inserting the last result into (51) and using for the viscous term at the right side the same approximation as in Equation (42), we obtain:

$$\frac{dI^*}{d\omega_o t} - \frac{20}{13} k_{to} \left(\frac{\omega}{\omega_o}\right)^{9/5} = \frac{8}{(Re)_o} \left(\frac{\omega}{\omega_o}\right) \left[\frac{1}{I^*} \frac{\omega}{\omega_o} - 1\right] \qquad (52)$$

where again $(Re)_o = \frac{a^2 \omega_o}{\nu}$ and $k_{to} = 0.035 \left(\frac{2a}{h}\right) (Re_o)^{-1/5}$

In order to evaluate the integral in Equation (51) for later times, when the assumption $r \approx a$ is no longer valid, we have to make assumptions about the shape of the velocity profiles $v_o(r)$. We may assume, that the velocity profiles are

given again roughly by Equation (32). These profiles, at least, satisfy the compatibility condition (33), i.e., they are correct near the wall.

Using the v_o profiles given by (32) the integral in Equation (51) can be evaluated and expressed by I*. After some lengthy calculation, one finally obtains from Equation (51):

$$\frac{dI^*}{d\omega_o t} - k_{to}\left(\frac{\omega}{\omega_o}\right)^{9/5} \cdot \frac{\left(1 - I^*\frac{\omega_o}{\omega}\right)^{8/5}}{\left(I^*\frac{\omega_o}{\omega}\right)^{13/5}} \cdot 4\int_0^{I^*\left(\frac{\omega_o}{\omega}\right)} \frac{x^{8/5}}{(1-x)^{3/10}}\,dx$$

$$= \frac{8}{Re_o}\frac{\omega}{\omega_o}\left[\frac{1}{I^*}\frac{\omega}{\omega_o} - 1\right] \qquad (53)$$

For small times, i.e., as long as $I^*\frac{\omega_o}{\omega} << 1$, the integral approximates to:

$$\approx \frac{5}{13}\left(I^*\frac{\omega_o}{\omega}\right)^{13/5},$$

while $\left(1 - I^*\frac{\omega_o}{\omega}\right)^{8/5} \approx 1$, and Equation (53) reduces to Equation (52).

Equation (53) has been used to calculate the spin decay of liquid-filled shell for $Re_o > 3.10^5$.

III. COMPARISON WITH EXPERIMENTS

In order to test the analysis given in the preceding section, some of the theoretical predictions have been compared with existing experimental data.

A detailed description of the experimental arrangements is given by Karpov (1962).

A quantity which has been measured directly is the axial spin decay of liquid-filled shells, fired from a gun. After the shell leaves the gun, the angular velocity decreases continuously. The decrease of angular velocity is caused by absorption of angular momentum in the liquid and by the torque due to air friction. The contribution of the air friction, which is usually small, can be determined separately by observation of the spin decrease of the empty shell. The difference, which is due to absorption of angular momentum has been plotted for two typical cases in Figure 4 and Figure 5. For comparison, the theoretical curves are plotted in the same diagram and also the curves obtained from the theory without secondary flow. The fineness ratio of the cylindrical cavity was in both cases $\frac{h}{2a} = 2.68$. For fineness ratios smaller than 2.68 the effect of the secondary flow would be even more pronounced.

The Reynolds number for the case plotted in Figure 4 was Re = 1.76×10^5 so that a laminar boundary layer flow could be assumed, while for the case of Figure 5 the Reynolds number of Re = 6.1×10^5 was above critical and therefore the formula for turbulent boundary layer flow was applied.

In addition to observations of spin decay, experiments have been done to observe the secondary flow itself. To this end an impulsive spin generator was designed which is described by Stoller (1960). The spin generator consisted of a liquid-filled cylinder with transparent walls which could be started impulsively to spin about its axis. A suspension of small particles was dissolved in the liquid, the specific gravity of the particles being the same as that of the liquid. The trajectories of the particles could be observed with the aid of a motion camera. For this type of observation, of course, only transparent liquids could be used.

Figure 6 shows some of the observed particle trajectories, or rather the first part of it, and the particle positions at constant time intervals. Close to the observed trajectories, theoretical trajectories and particle positions according to Equation (25) are plotted. The agreement is reasonably good. Some deviations can be explained by the fact that the Reynolds number of the experimental flow was rather low (Re = 1.83×10^4) while the theoretical prediction is based on the assumption of high Reynolds numbers, where the viscous forces in the core flow can be neglected.

ACKNOWLEDGMENT

The author is grateful to Dr. F. D. Bennett and Dr. R. Sedney for advice and helpful discussions, and to Dr. B. G. Karpov, who made the experimental data accessible.

E. H. Wedemeyer.

E. H. WEDEMEYER

REFERENCES

1. Stewartson, K., J. Fluid Mech 5, Part 4, 1959.
2. Karpov, B. G., BRL Report No. 1171, 1962.
3. Ludwieg, H., Ingenieur-Archiv 19, 296, 1951.
4. Thiriot, K. H., ZAMM 20, 1, 1940.
5. von Kármán, T. ZAMM 1, 233, 1921.
6. Cochran, W. G., Proceedings of the Cambridge Phil. Society 30, 365, 1934.
7. Bödewadt, U. T., ZAMM 20, 241, 1940.
8. Batchelor, G. K., Quart. J. Mech. Appl. Math. 4, 29, 1951.
9. Stewartson, K., Boundary Layer Research Symposium, 1958, Freiburg, 59-71, 1957; Springer Verlag, Berlin, 1958.
10. Rogers, M. H. and Lance, G. N., J. Fluid Mech 7, 617, 1960.
11. Squire, H. B., ARC 16,021, 1953.
12. Mack, L. M., Jet Propulsion Lab., Pasadena, California, Tech Rep 32-224, 1962.
13. Mack, L. M., Jet Propulsion Lab., Pasadena, California, Tech Rep 32-366, 1963.
14. Schlichting, H., Grenzschicht-Theorie, Verlag G. Braun, Karlsruhe (1958).
15. Stoller, H. M., BRL Tech Note. 1355, 1960.

FIG. 1

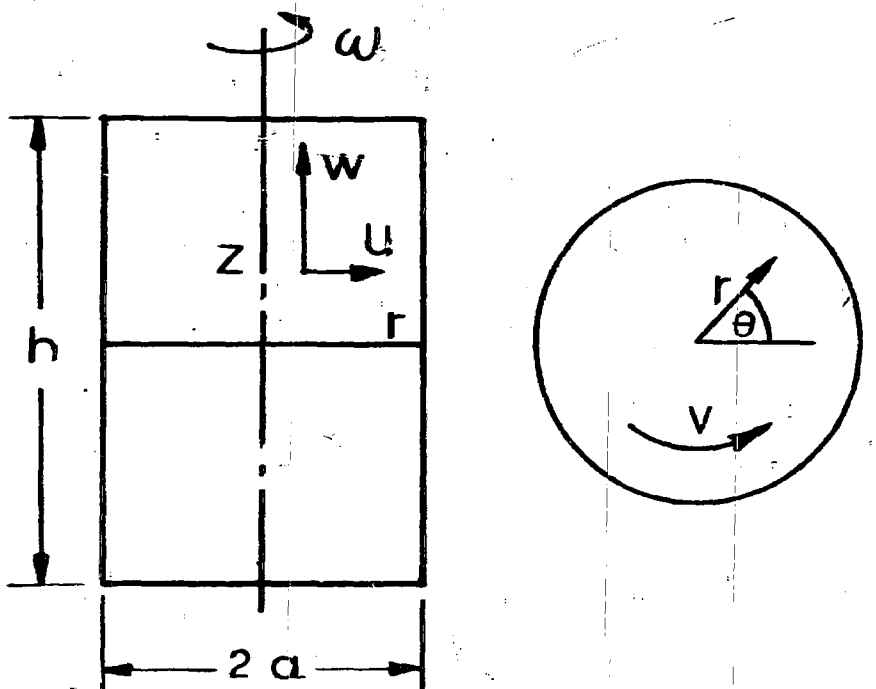

Axial Section and Cross Section of Spinning Cylinder.

FIG. 2

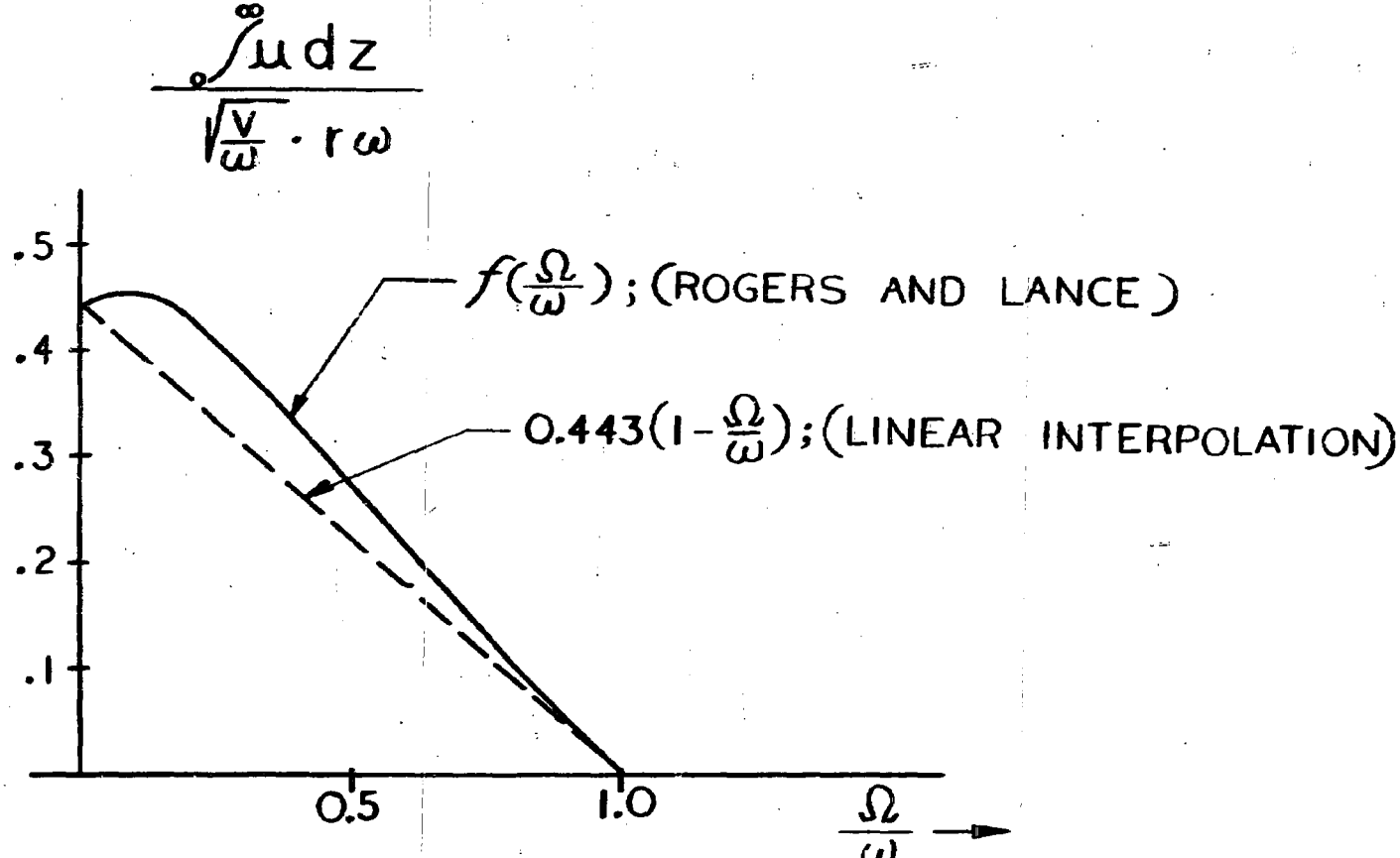

Radial Flow Integral as a Function of $\frac{\Omega}{\omega}$. Solid Line: Rogers and Lance (Exact). Dotted Line: Linear Interpolation $[0.443\ (1 - \frac{\Omega}{\omega})]$.

FIG. 3

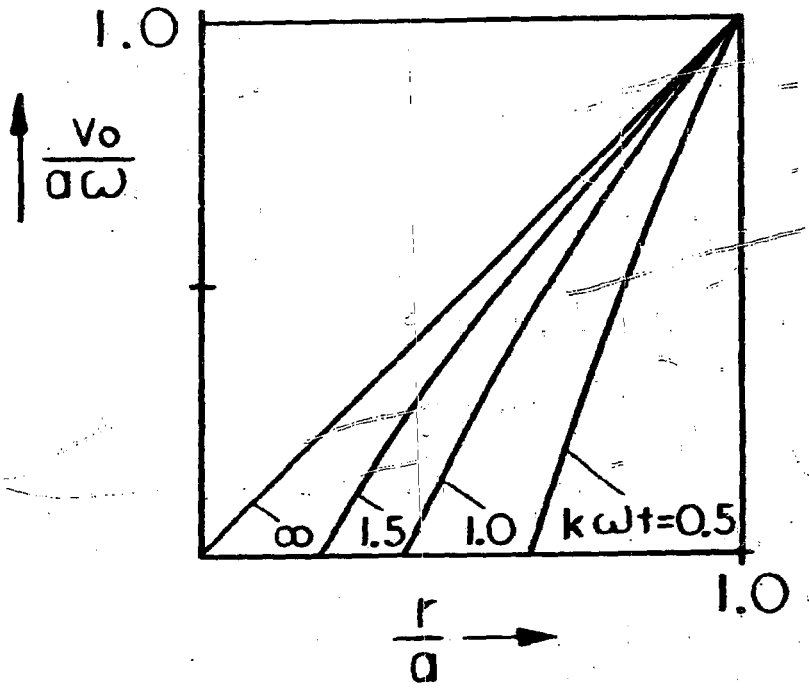

Velocity Profiles for the Core Flow.

FIG. 4

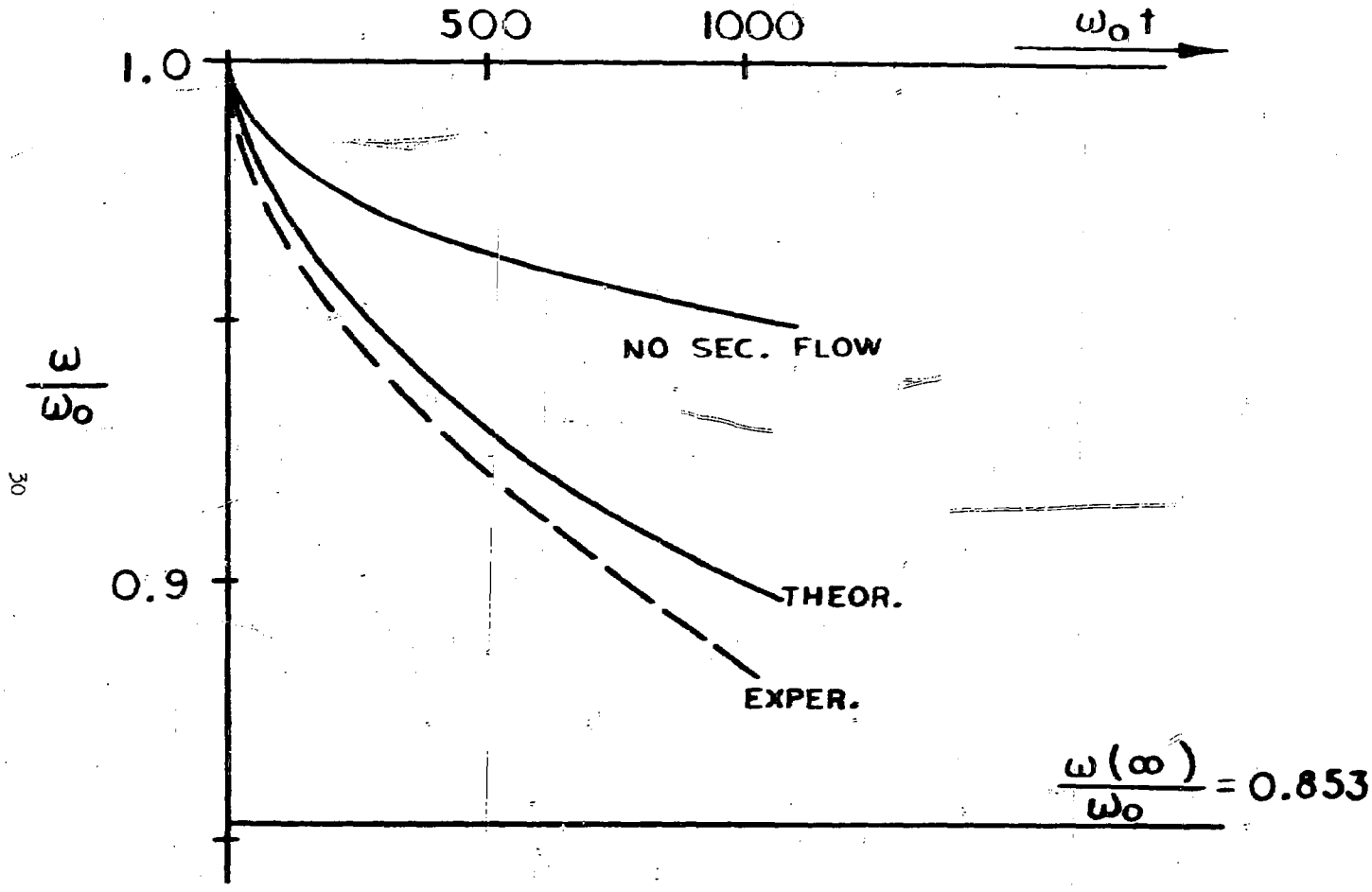

Spin Decay for Laminar Boundary Layer Flow. $Re = 1.76 \times 10^5$, $\frac{h}{2a} = 2.68$.

FIG. 5

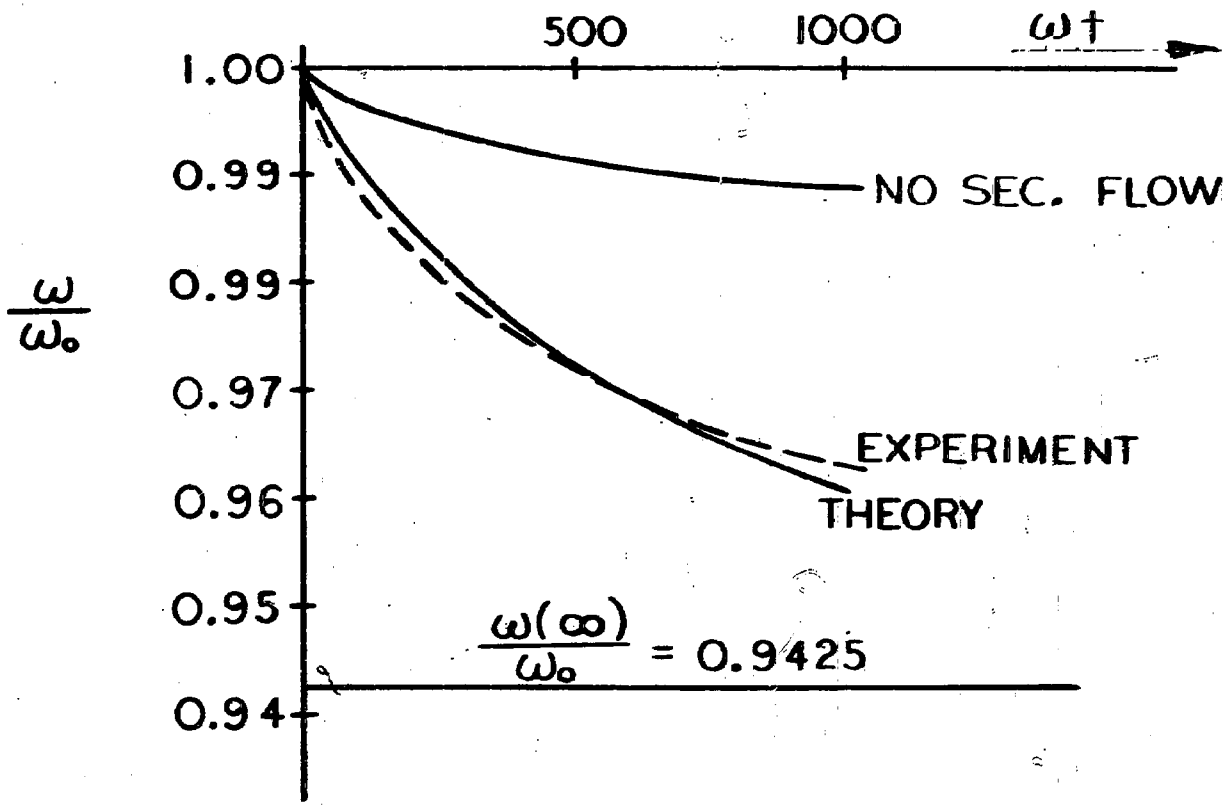

Spin Decay for Turbulent Boundary Layer Flow. $Re = 6.1 \times 10^5$, $\frac{h}{2a} = 2.68$.

FIG. 6

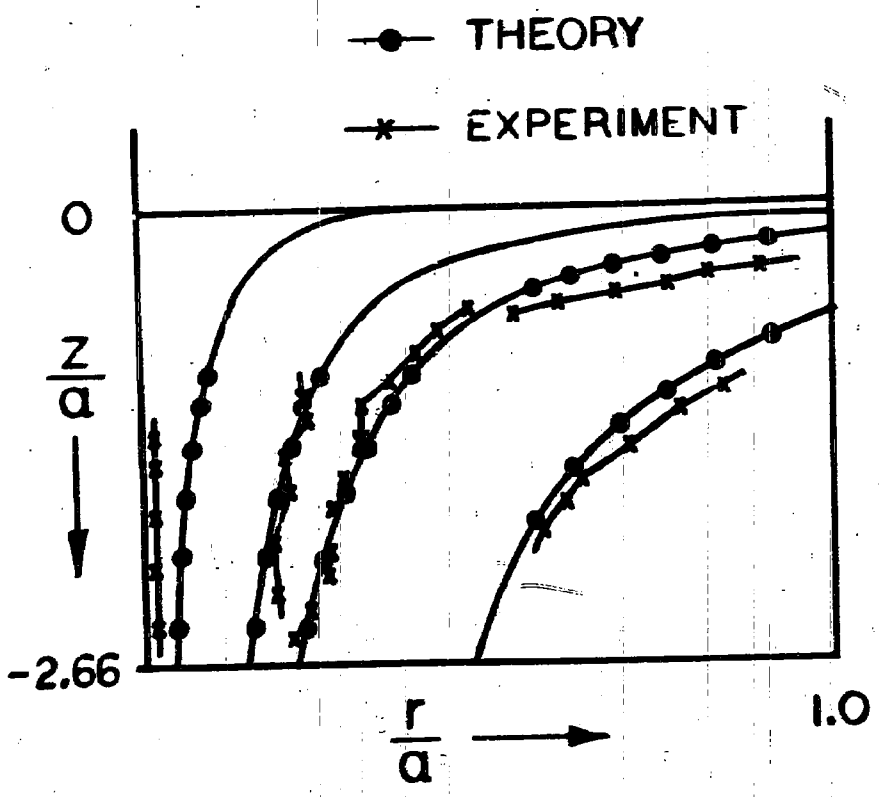

Particle Trajectories and Position of Particles at 0.25 Sec. Intervals.

DISTRIBUTION LIST

No. of Copies	Organization
20	Commander Defense Documentation Center ATTN: TIPCR Cameron Station Alexandria, Virginia 22314
1	Chief, Defense Atomic Support Agency Washington, D. C. 20301
1	Director of Defense Research and Engineering (OSD) Director/Ordnance Washington, D. C. 20301
1	Commanding General U. S. Army Materiel Command ATTN: AMCRD-RP-B Washington, D. C. 20315
2	Commanding Officer Frankford Arsenal ATTN: Library Branch, 0270, Bldg. 40 Philadelphia, Pennsylvania 19137
3	Commanding Officer Picatinny Arsenal Dover, New Jersey 07801
2	Commanding General U. S. Army Missile Command Redstone Arsenal, Alabama 35808
1	Commanding Officer Fort Detrick Frederick, Maryland 21701
1	Professor of Ordnance U. S. Military Academy West Point, New York 10996
1	Army Research Office 3045 Columbia Pike Arlington, Virginia
3	Chief, Bureau of Naval Weapons ATTN: DLI-3 Department of the Navy Washington, D. C. 20360
2	Commander U. S. Naval Ordnance Laboratory White Oak Silver Spring 19, Maryland
1	Commander U. S. Naval Ordnance Test Station ATTN: Technical Library China Lake, California 93557
1	Library U. S. Naval Postgraduate School ATTN: Technical Reports Section Monterey, California
1	Commander U. S. Naval Weapons Laboratory Dahlgren, Virginia 22448
2	Commander U. S. Naval Missile Center Point Mugu, California 93041
1	Commanding Officer U. S. Naval Air Development Center Johnsville, Pennsylvania
1	Commanding Officer U. S. Naval Ammunition and Net Depot ATTN: Technical Services Library, AO-2 Seal Beach, California

DISTRIBUTION LIST

No. of Copies	Organization
1	Chief of Naval Research Department of the Navy Washington, D. C. 20360
1	Commanding Officer and Director David W. Taylor Model Basin ATTN: Aerodynamics Laboratory Washington, D. C. 20007
1	Hq, USAF (AFCOA, RST) Washington, D. C. 20330
1	AEDC Arnold Air Force Station Tennessee
1	AFFDL Wright-Patterson Air Force Base Ohio
1	Scientific & Technical Information Facility ATTN: NASA Representative (S-AK-DL) P.O. Box 5700 Bethesda, Maryland 20014
5	Director National Aeronautics and Space Administration ATTN: Division Research Information 1520 H Street, N. W. Washington, D. C. 20546
2	Director National Aeronautics and Space Administration ATTN: Dr. A. C. Charters Mr. H. J. Allen Ames Research Center Moffett Field, California
2	U. S. Atomic Energy Commission Sandia Corporation ATTN: Mrs. Wynne K. Cox P.O. Box 5800 Albuquerque, New Mexico 87115
2	Applied Physics Laboratory The Johns Hopkins University 8621 Georgia Avenue Silver Spring, Maryland
3	Jet Propulsion Laboratory ATTN: Reports Group (2 cys) Mr. J. Lorell 4800 Oak Grove Drive Pasadena, California 91103
1	Aerojet-General Corporation Azusa, California
1	Aerojet-General Corporation ATTN: H. A. Kuerschner Ord Systems Department P.O. Box 458 Goleta, California
1	Arthur D. Little, Inc. Acorn Park Cambridge 40, Massachusetts
1	Bendix Mishawaka Division Bendix Aviation Corporation 400 South Beiger Street Mishawaka, Indiana
1	Chance Vought Aircraft Corporation P.O. Box 5907 Dallas, Texas
1	CONVAIR, A Division of General Dynamics Corporation Fort Worth 1, Texas

DISTRIBUTION LIST

No. of Copies	Organization
1	CONVAIR, A Division of General Dynamics Corporation Guided Missile Division Pomona, California
1	Cornell Aeronautical Laboratory, Inc. ATTN: Mr. Joseph Desmond, Librarian Buffalo 21, New York
1	Wright Aeronautical Division Curtiss-Wright Corporation ATTN: Sales Department (Gov't) Wood-Ridge, New Jersey
1	Douglas Aircraft Company 300 Ocean Park Boulevard Santa Monica, California
1	Eastman Kodak Company Rochester 4, New York
1	Fairchild Engine and Airplane Corporation Guided Missile Division ATTN: W. J. McDonald, Librarian Wyandanch, Long Island, New York
1	Goodyear Aircraft Corporation Akron 15, Ohio
1	Grumman Aircraft Engineering Corporation Bethpage, Long Island New York
1	Hughes Aircraft Company Florence Ave. at Teal Street Culver City, California
1	Marquardt Aircraft Company ATTN: Mr. Robert E. Marquardt 16555 Saticoy Street P.O. Box 2013 South Annex Van Nuys, California
1	The Martin Company Baltimore 3, Maryland
1	McDonnell Aircraft Corporation ATTN: Dr. B. G. Bromberg P.O. Box 516 St. Louis 3, Missouri
1	NORAIR, A Division of Northrop Corporation 1001 East Broadway Hawthorne, California 90250
2	North American Aviation, Inc. Space & Information Systems Division ATTN: Technical Information Center Aerophysics Library 12214 Lakewood Boulevard Downey, California 90241
1	Raytheon Manufacturing Company ATTN: Guided Missiles and Radar Division Waltham, Massachusetts
1	Republic Aviation Corporation Military Contract Department ATTN: Dr. William O'Donnell Farmingdale, Long Island New York
1	Sperry Gyroscope Company Division of the Sperry Corporation ATTN: Librarian Great Neck, Long Island New York

DISTRIBUTION LIST

No. of Copies	Organization
1	United Aircraft Corporation Research Department ATTN: Mr. Robert C. Sale East Hartford 8, Connecticut
2	Illinois Institute of Technology ATTN: Document Library 10 West 35th Street Chicago 16, Illinois
1	The Johns Hopkins University Institute for Cooperative Research ATTN: Project THOR 3506 Greenway Baltimore, Maryland 21218
2	Massachusetts Institute of Technology ATTN: Guided Missiles Library Room 22-001 Cambridge 39, Massachusetts
1	Purdue University ATTN: Dr. M. J. Zucrow Lafayette, Indiana
1	Southwest Research Institute ATTN: Dr. Norman Abramson 8500 Culebra Road P.O. Box 2296 San Antonio 6, Texas
1	University of Michigan Willow Run Laboratories P.O. Box 2008 Ann Arbor, Michigan [illegible]
1	University of Southern California Naval Research Project ATTN: Mr. R. T. DeVault College of Engineering Los Angeles 7, California
1	University of Texas Defense Research Laboratory ATTN: Dr. C. P. Boner P.O. Box 8029 University Station Austin, Texas
1	Professor George Carrier Harvard University Division of Engineering and Applied Physics Cambridge 38, Massachusetts
1	Professor Edward J. McShane University of Virginia Department of Mathematics Charlottesville, Virginia
1	Dr. Y. H. Pao Boeing Scientific Research Lab P.O. Box 3981 Seattle, Washington
1	Dr. L. H. Thomas Watson Scientific Computing Lab 612 West 116th Street New York 25, New York
1	Mr. H. F. Bauer (M-AERO-D) Marshall Research Center Redstone Arsenal, Alabama 35808

DISTRIBUTION LIST

No. of Copies	Organization
1	Mr. Joseph I. Bluhan Watertown Arsenal Watertown, Massachusetts 02172
1	Mr. J. E. Brooks Space Technology Laboratories, Inc. Airport Office Building 8929 Sepulveda Boulevard Los Angeles, California
1	Mr. Harry O. Hass Engineering Progress Coordinator U. S. Army Chemical Corps Engineering Command Edgewood Arsenal, Maryland 21040
1	Professor K. Stewartson University of Durham Department of Mathematics Science Laboratories South Road Durham City, England
4	Australian Group c/o Military Attache Australian Embassy 2001 Connecticut Avenue, N.W. Washington, D. C.
10	The Scientific Information Officer Defence Research Staff British Embassy 3100 Massachusetts Avenue, N.W. Washington, D. C. 20008
4	Defence Research Member Canadian Joint Staff 2450 Massachusetts Avenue, N.W. Washington, D. C. 20008
	Aberdeen Proving Ground
	Chief, TIB
	Air Force Liaison Office Marine Corps Liaison Office Navy Liaison Office CDC Liaison Office
	D & PS Branch Library
	Information Office - Pvt. Mearns

AD Accession No.
Ballistic Research Laboratories, APG
THE UNSTEADY FLOW WITHIN A SPINNING CYLINDER
E. H. Wedemeyer

BRL Report No. 1225 October 1963

RDT & E Project No. 1M010501A005
UNCLASSIFIED Report

UNCLASSIFIED

Bodies of revolution - Stability
Liquid-filled shell - Stability

A theoretical analysis is given of the unsteady flow within a liquid-filled cylinder of finite length, which is started impulsively to spin about its axis.

It is established that a secondary flow, which is caused by the cylinder ends, has a remarkable effect on the generation of spin in the liquid.

The theoretical results are compared with experimental observations and good agreement is found.

AD Accession No.
Ballistic Research Laboratories, APG
THE UNSTEADY FLOW WITHIN A SPINNING CYLINDER
E. H. Wedemeyer

BRL Report No. 1225 October 1963

RDT & E Project No. 1M010501A005
UNCLASSIFIED Report

UNCLASSIFIED

Bodies of revolution - Stability
Liquid-filled shell - Stability

A theoretical analysis is given of the unsteady flow within a liquid-filled cylinder of finite length, which is started impulsively to spin about its axis.

It is established that a secondary flow, which is caused by the cylinder ends, has a remarkable effect on the generation of spin in the liquid.

The theoretical results are compared with experimental observations and good agreement is found.

AD Accession No.
Ballistic Research Laboratories, APG
THE UNSTEADY FLOW WITHIN A SPINNING CYLINDER
E. H. Wedemeyer

BRL Report No. 1225 October 1963

RDT & E Project No. 1M010501A005
UNCLASSIFIED Report

UNCLASSIFIED

Bodies of revolution - Stability
Liquid-filled shell - Stability

A theoretical analysis is given of the unsteady flow within a liquid-filled cylinder of finite length, which is started impulsively to spin about its axis.

It is established that a secondary flow, which is caused by the cylinder ends, has a remarkable effect on the generation of spin in the liquid.

The theoretical results are compared with experimental observations and good agreement is found.

AD Accession No.
Ballistic Research Laboratories, APG
THE UNSTEADY FLOW WITHIN A SPINNING CYLINDER
E. H. Wedemeyer

BRL Report No. 1225 October 1963

RDT & E Project No. 1M010501A005
UNCLASSIFIED Report

UNCLASSIFIED

Bodies of revolution - Stability
Liquid-filled shell - Stability

A theoretical analysis is given of the unsteady flow within a liquid-filled cylinder of finite length, which is started impulsively to spin about its axis.

It is established that a secondary flow, which is caused by the cylinder ends, has a remarkable effect on the generation of spin in the liquid.

The theoretical results are compared with experimental observations and good agreement is found.